CMS Papers

Transverse-momentum and pseudorapidity distributions of charged hadrons in pp collisions at

Sqrt(s) = 7 TeV

Abstract

- Measurements of inclusive charged-hadron transverse-momentum and pseudorapidity distributions.
- For non-single-difractive interactions, the average charged-hadron transverse momentum is measured
  - 0.46 ± 0.01 (stat.) ± 0.01 (syst.) GeV/c at 0.9 TeV and
  - 0.50 ± 0.01 (stat.) ± 0.01 (syst.) GeV/c at 2.36 TeV,
  - 0.545 ± 0.005 (stat.) ± 0.015 (syst.) GeV/c at 7 TeV

  for pseudorapidities between – 2.4 and +2.4.
- Measured pseudorapidity densities in the central region, dNch=d\eta (|\eta|<0:5)
  - 3.48 ± 0.02 (stat.) ± 0.13 (syst.)
  - 4.47 ± 0.04 (stat.) ± 0.16 (syst.),
  - 5.82 ± 0.01 (stat.) ± 0.23 (syst.),

Introduction

- The majority of pp collisions are soft, i.e., without any hard scattering of the partonic constituents of the proton. In contrast to the higher-pT regime, well described by perturbative QCD, particle production in soft collisions is generally modelled phenomenologically to describe the dierent pp scattering processes: elastic scattering, single-diractive and double-diractive dissociation, and inelastic non-difractive scattering

$$(dN_{\mathrm{ch}}/dp_{\mathrm{T}} \text{ and } dN_{\mathrm{ch}}/d\eta) \qquad |\eta| < 2.4,$$

  - pT is the momentum of the particle transverse to the beam axis,
  - Nch is the number of charged hadrons in any given eta or pT interval
- Important for understanding the mechanisms of hadron production and the relative roles of soft and hard scattering contributions in the LHC energy regime.
- Primary charged hadrons:
  - Defined as all charged hadrons produced in the interactions, including the products of strong and electromagnetic decays, but excluding products of weak decays and hadrons originating from secondary interactions.

- Soft collisions are usually divided into several categories, namely elastic scattering, inelastic single-diffractive (SD) and double-diffractive (DD) dissociation, and inelastic non-diffractive (ND) scattering
- Multiplicity densities are measured for
  - Inelastic non-single-difractive (NSD) interactions to minimize the model dependence of the necessary corrections for the event selection, and to enable a comparison with earlier experiments.
- Event selection designed to retain large fraction of
  - inelastic double-difractive (DD) and
  - non-difractive (ND) events,
- while rejecting
  - all elastic and
  - most single-diractive dissociation (SD) events.

Table 1: Number of events used in this analysis. The selection criteria are applied in sequence, i.e., each line includes the selection of the lines above.

Selection	Number of Events
BPTX Coincidence + one BSC Signal	243 938
Valid Event Vertex	208 966
HF Coincidence	186 833
Beam Halo Rejection	186 796
Beam Background Rejection	186 771

The event selection and analysis methods in this paper are identical to those used in Ref. [5], where more details can be found. The inelastic pp collision rate was about 50 Hz, and the probability for more than one collision to occur in the same bunch crossing is less than 0.5%. The coincidence between any hit in the Beam Scintillator Counters (BSCs) covering the range $3.23 < |\eta| < 4.65$, and the Beam Pick-up Timing for the eXperiments (BPTX) devices, was

The fraction of background events in the data after selections was estimated from unpaired-bunch data to be less than $2 \times 10{-}5$.

MC and Reco

	PYTHIA				PHOJET			
Energy	0.9 TeV		2.36 TeV		0.9 TeV		2.36 TeV	
	Frac.	Sel. Eff.	Frac.	Sel. Eff.	Frac.	Sel. Eff.	Frac.	Sel. Eff.
SD	22.5%	16.1%	21.0%	21.8%	18.9%	20.1%	16.2%	25.1%
DD	12.3%	35.0%	12.8%	33.8%	8.4%	53.8%	7.3%	50.0%
ND	65.2%	95.2%	66.2%	96.4%	72.7%	94.7%	76.5%	96.5%
NSD	77.5%	85.6%	79.0%	86.2%	81.1%	90.5%	83.8%	92.4%

	PYTHIA		PHOJET	
	Frac.	Sel. Eff.	Frac.	Sel. Eff.
SD	19.2%	26.7%	13.8%	30.7%
DD	12.9%	33.6%	6.6%	48.3%
ND	67.8%	96.4%	79.5%	97.1%
NSD	80.8%	86.3%	86.2%	93.4%

- Rapidity distribution = counting of
  - (i) reconstructed clusters in the pixel barrel detector;
  - (ii) pixel tracklets composed of pairs of clusters in dierent pixel barrel layers; and
  - (iii) tracks reconstructed in the full tracker volume, combining the pixel and strip hits.

$$E\frac{d^3N_{\mathrm{ch}}}{dp^3} = \frac{1}{2\pi p_T}\frac{E}{p}\frac{d^2N_{\mathrm{ch}}}{d\eta dp_T} = C\frac{dN_{\mathrm{ch}}}{dy}\left(1+\frac{E_T}{nT}\right)^{-n}$$

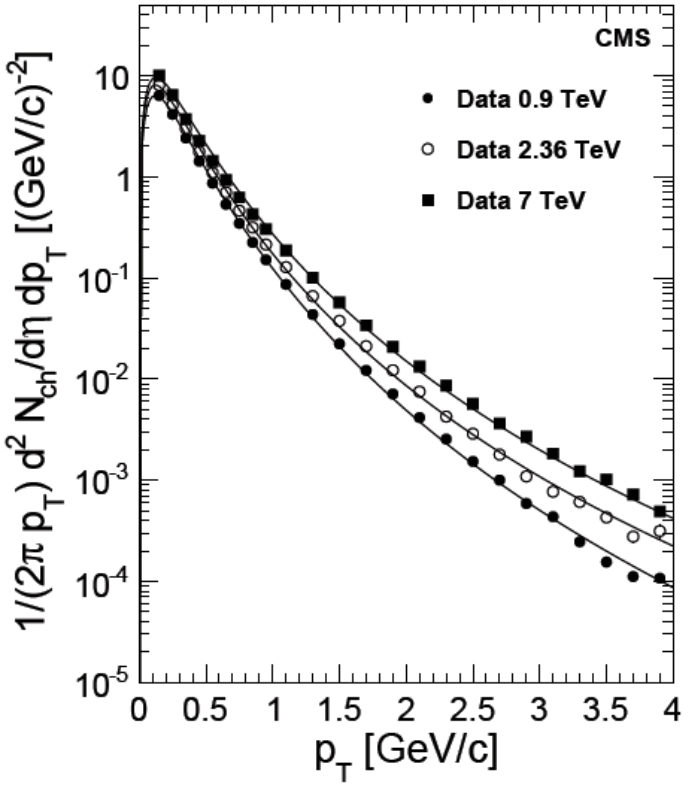

Figure 2: Measured yield of charged hadrons for $|\eta| < 2.4$ with systematic uncertainties (symbols), together with the empirical fits (Eq. 1).

where $y = 0.5\ln[(E+p_z)/(E-p_z)]$ is the rapidity; C is a normalization constant, $E_T = \sqrt{m^2+p_T^2}-m$, and m is the π^+ mass. The p_T spectrum of charged hadrons, $1/(2\pi p_T)d^2N_{\mathrm{ch}}/d\eta dp_T$, in the full measured region $|\eta| < 2.4$, is shown in Fig. 2 with fit results to Eq. 1. The inverse slope parameter T and the exponent n were found to be $T = 0.145 \pm 0.005$ (syst.) GeV and $n = 6.6 \pm 0.2$ (syst.). The average transverse momentum, calculated from the measured data points and adding the low- and high-p_T extrapolations from the fit is $\langle p_T \rangle = 0.545 \pm 0.005$ (stat.) $\pm$ 0.015 (syst.) GeV/c, significantly below the predicted value of 0.59 GeV/c from [14].

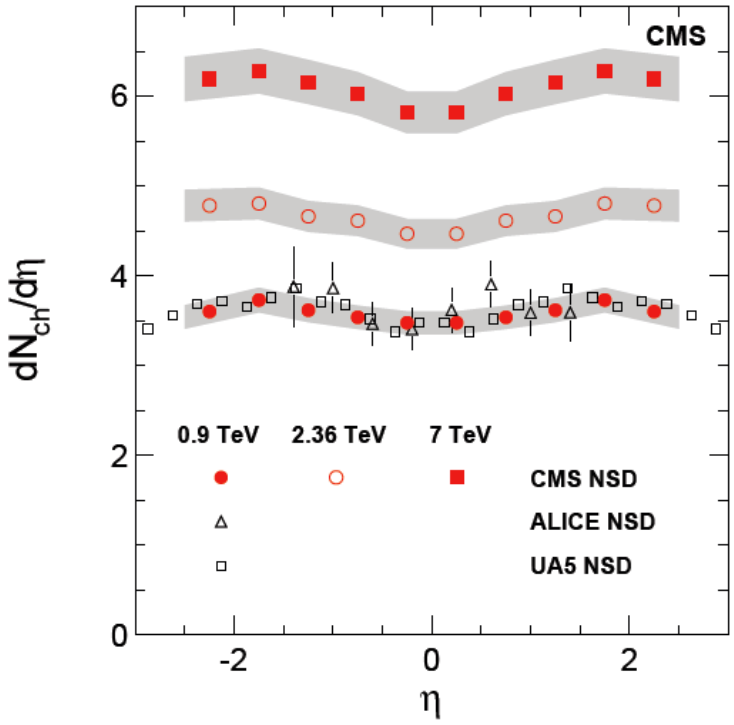

Figure 3: (color online) $dN_{ch}/d\eta$ distributions averaged over the analysis methods (circles), compared to data from UA5 [15] (open squares) and ALICE [16] (open triangles). The shaded band shows systematic uncertainties.

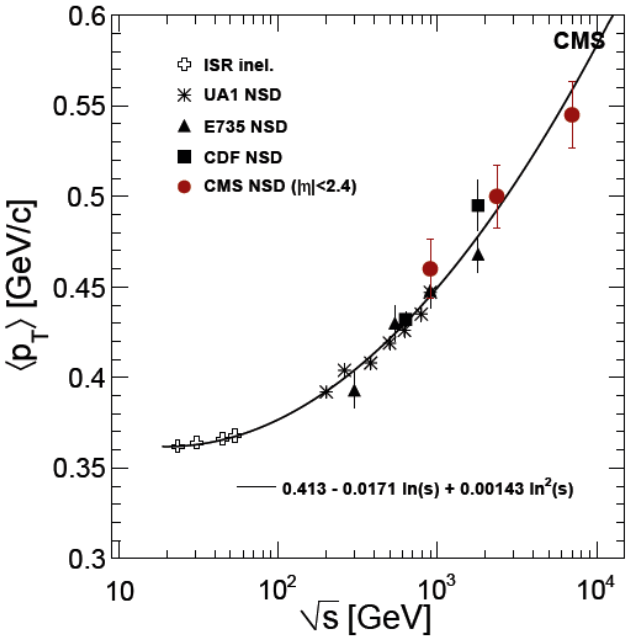

Figure 4: (color online) Energy dependence of $\langle p_T \rangle$ of charged hadrons. The CMS data are evaluated for $|\eta| < 2.4$. Data of other experiments are from [17–20]. The curve shown is of the form $\langle p_T \rangle = 0.409 - 0.0163 \ln(s) + 0.00139 \ln^2(s)$. The error bars on the CMS data points include systematic uncertainties.

(called also Tsallis distributions)[2]:

$$\exp\left(-\frac{X}{\lambda}\right) \Rightarrow \exp_q\left(-\frac{X}{\lambda}\right) = \left[1-(1-q)\frac{X}{\lambda}\right]^{\frac{1}{1-q}}$$

1/1-q → -n

$$E\frac{d^3N_{\rm ch}}{dp^3} = \frac{1}{2\pi p_T}\frac{E}{p}\frac{d^2N_{\rm ch}}{d\eta dp_T} = C(n,T,m)\frac{dN_{\rm ch}}{dy}\left(1+\frac{E_T}{nT}\right)^{-n},$$

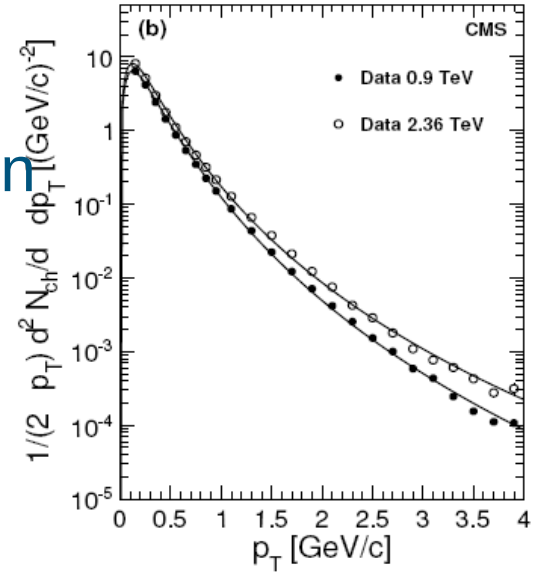

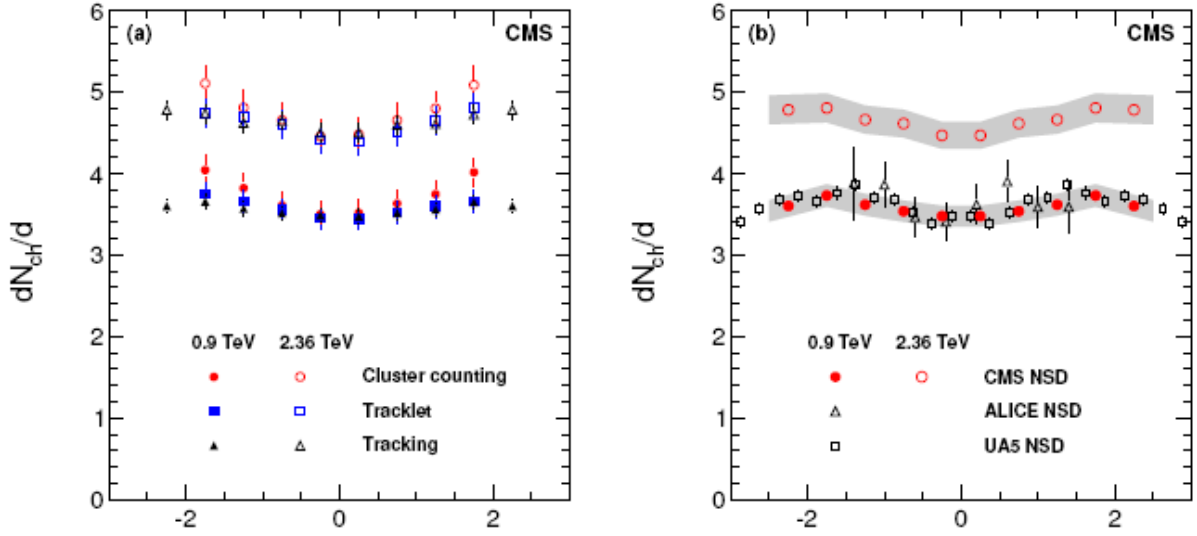

Figure 6. (a) Reconstructed $dN_{\rm ch}/d\eta$ distributions obtained from the cluster counting (dots with error bars), tracklet (squares) and tracking (triangles) methods, in pp collisions at 0.9 TeV (filled symbols) and 2.36 TeV (open symbols). The error bars include systematic uncertainties (as discussed in the text), excluding those common to all the methods. (b) Reconstructed $dN_{\rm ch}/d\eta$ distributions averaged over the cluster counting, tracklet and tracking methods (circles), compared to data from the UA5 [24] (open squares) and from the ALICE [23] (open triangles) experiments at 0.9 TeV, and the averaged result over the three methods at 2.36 TeV (open circles). The CMS and UA5 data points are symmetrized in η. The shaded band represents systematic uncertainties of this measurement, which are largely correlated point-to-point. The error bars on the UA5 and ALICE data points are statistical only.

Kinematics - Rapidity

- One Body Phase Space
- Non Relativistic

$$d\vec{P} = P^2 dP d\Omega = dP_{\parallel} P_T dP_T d\phi$$

Relativistic

$$d^4P\, d\left(P^2 - m^2\right) = d\vec{P} / E$$

$$= \pi dy d\left(P_T^2\right)$$

$$dy = dP_{\parallel} / E$$

If transverse momentum is limited by dynamics, expect a uniform distribution in y

Rapidity

$$E = m_T \cosh y$$

$$m_T^2 = m^2 + P_T^2$$

$$\max y \; at \; P_T = 0, beam\; momentum$$

$$pp @ 2, \quad 14\, TeV,$$

$$y_{\max} = 7.7, \quad 9.6$$

Kinematically allowed range in y of a proton with P_T=0

Rapidity “Plateau”

Monte Carlo results are from COMPHEP - running under Windows or Linux

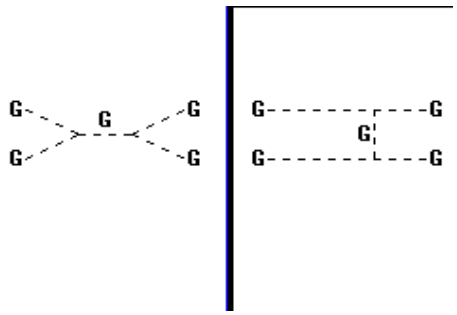

Region around y=0 (90 degrees) has a “plateau” with width Δy ~ 6 for LHC

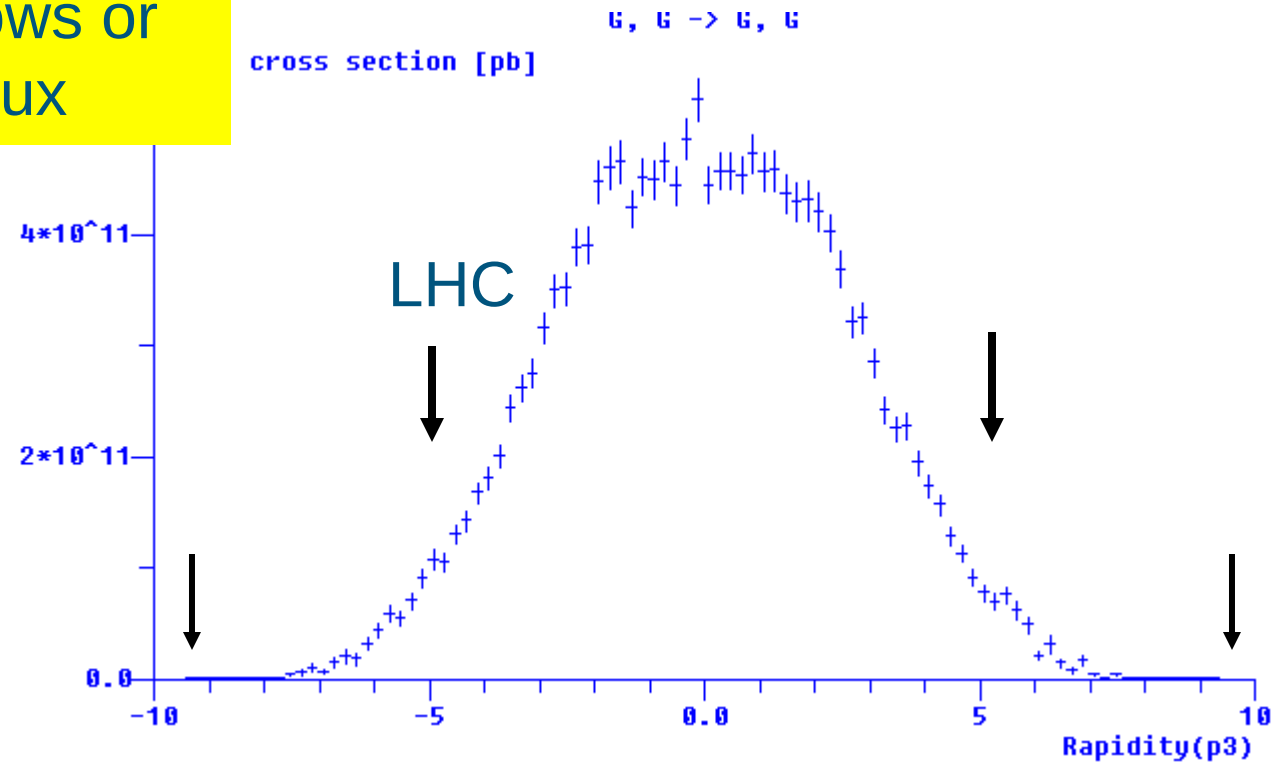

Rapidity Plateau - Tevatron

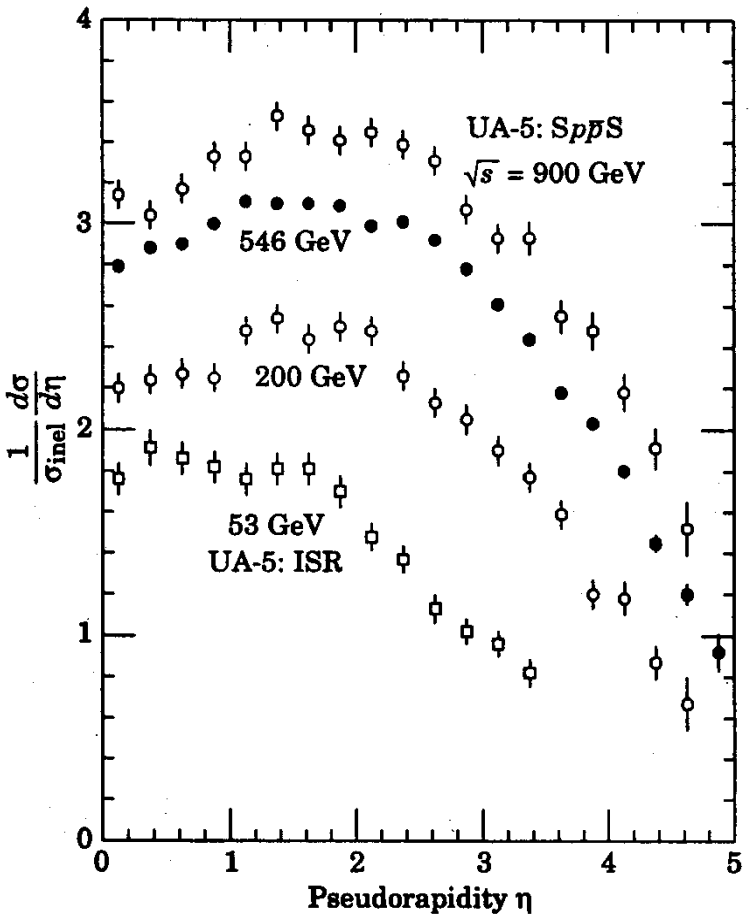

Existing data exhibits a plateau in rapidity.